Available online at www.sciencedirect.com

ScienceDirect

Nuclear Instruments and Methods in Physics Research B 263 (2007) 271–278

NIM B
Beam Interactions with Materials & Atoms

www.elsevier.com/locate/nimb

Optical appearance of alpha particle tracks in CR-39 SSNTD

K.N. Yu *, H.H.W. Lee, A.W.T. Wong, Y.L. Law, S.F.L. Cheung, D. Nikezic, F.M.F. Ng

Department of Physics and Materials Science, City University of Hong Kong, Tat Chee Avenue, Kowloon Tong, Kowloon, Hong Kong

Abstract

A ray tracing method based on geometrical optics was used to study the tracks from alpha particles with different energies and with an incident angle of 50°. The transmission operation mode of the microscope is simulated. Considering the distribution of light intensities from the tracks, the mean and the 80% percentile gray levels from real experiments are proposed as quantitative variables to differentiate among tracks. The gray level properties for the same track for different exposures can vary to large extents. We introduce three variables, κ, λ and ε, to make empirical corrections. It is interesting to see that these coefficients are very consistent for the same alpha particle track despite the very different gray level properties. Gray level results have been obtained for tracks from alpha particles with 50° incident angle and different incident energies. However, the track depths cannot be predicted by any one of the coefficients κ, λ and ε. Multivariate analyses can help separate the tracks corresponding to different alpha energies. By using discriminant analysis with κ, λ and ε as independents, effectively all alpha energies can be determined with an accuracy of ±0.5 MeV.

PACS: 29.40; 23.60

Keywords: CR-39 detector; Alpha particles; Tracks; Ray tracing; Gray level

1. Introduction

One of the challenging tasks in the application of solid-state nuclear track detectors (SSNTDs) is the automation in differentiating among recorded tracks due to alpha particles with different incident energies. This will be very useful in, for example, the studies of airborne radon progeny [1]. One promising approach is to make use of the optical appearance of alpha particle tracks, such as the gray level properties.

Although the optical microscope was the main tool for track observation for many years, there has been relatively little investigation about the optical characteristics of the etched tracks. Only a few papers on this topic have appeared until now. For example, the "mean optical density" measured by an image analysis system as an additional parameter in track studies to extend the data available for α particles and protons [2]. An "average brightness" of a single track was also introduced to distinguish among various types of charged-particle tracks [3]. The optical properties of a single track obtained by neutron radiography was also discussed by Assunção et al. [4]. Skvarc [5] used a software package called POV-Ray (www.pov-ray.com) for simulation and rendering of the track images; and comparisons between simulated and measured tracks were given.

More recently, our group has performed a theoretical study of optical characteristics of tracks in the CR-39 SSNTD using the ray tracing method [6]. Based on geometrical optics, we developed our own computer program to simulate light propagation through the tracks and calculate the brightness of all grid elements in the track wall. The study revealed that the major factor affecting the track appearances was the total internal reflection and inclination angles of elements in the track wall with respect to the light rays. The ray tracing method was shown to be successful in generating realistic track images. For example, Fig. 1 shows a comparison between the images of the tracks for an alpha particle with 4.5 MeV incident energy

---

* Corresponding author. Tel.: +852 27887812; fax: +852 27887830.
E-mail address: peter.yu@cityu.edu.hk (K.N. Yu).

0168-583X/$ - see front matter © 2007 Elsevier B.V. All rights reserved.
doi:10.1016/j.nimb.2007.04.306

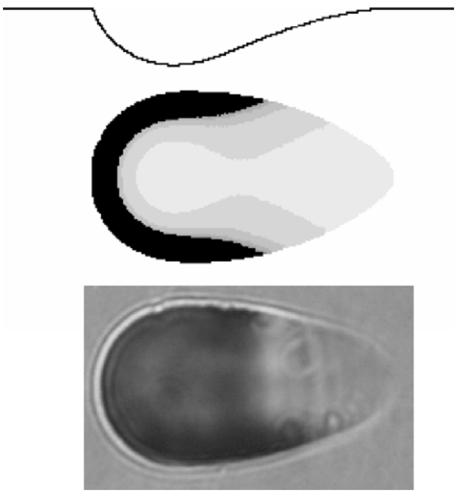

Fig. 1. Comparison between the simulated and experimentally recorded images of the tracks for an alpha particle with 4.5 MeV energy and 40° incident angle (after 15 h of etching at 70°C in 6.25 N NaOH). Top: The track profile determined by the *test* program. Middle: Image simulated using ray tracing. Bottom: Experimentally recorded image using an optical microscope in the transmission mode.

and 40° incident angle (with respect to the surface of the detector), which have been etched in 6.25 N aqueous NaOH for 15 h at 70 °C. The track profile determined by the *test* program (available on the webpage: www.cityu.edu.hk/ap/nru/test.htm) [7–9] is given on the top. The image simulated using ray tracing is given in the middle while the experimentally recorded image is given at the bottom. The spatial distributions of the gray levels in the two images agree qualitatively: both show the black rounded part on the left and both show a wide bright area from the centre of the track to the right end.

However, only qualitative comparisons have been made. For practical applications, e.g. in automation in differentiating among recorded tracks due to alpha particles with different incident energies, *quantitative* comparisons should be enabled. The first objective of the present paper is to theoretically show a screening method for tracks whose dimensions can be studied through light intensity properties. For some incidence angles, the tracks from different alpha energies might have no or very weak transmission of light, so that the light intensity is not useful for distinguishing alpha energies from these tracks. The second objective is to theoretically identify feasible variables based on light intensity properties which can be used for quantitative comparisons. We use the ray tracing method to obtain statistics on the light intensities of the tracks. Based on these data, we will identify the appropriate gray level properties as quantitative variables to differentiate among tracks.

The third objective will be to study the consistency of gray level properties of the tracks obtained through experiments. In particular, our experiments have shown that the average gray level for the same track might vary from one exposure to another. We will propose empirical corrections through the introduction of three coefficients, namely, κ, λ and ε, which are consistent for the same alpha particle track despite the very different gray level properties.

The fourth objective of the paper will be to study the gray level properties of the tracks obtained through experiments. As examples, the tracks from alpha particles with energies from 1.5 to 5 MeV and with an incident angle of 50° will be studied. The variation of track depths with κ, λ and ε will be studied. The tracks will also be studied using the scatter plot of factor scores (from factor analysis using κ, λ and ε as the variables) as well as discriminant analysis (with κ, λ and ε as independents).

2. Ray tracing

As described in the introduction, we will use the ray tracing method to obtain statistics on the light intensities of the tracks. As examples, the tracks from alpha particles with energies from 1.5 to 5 MeV (with steps of 0.5 MeV) and with incident angles of 90° and 50° will be employed for illustration of the idea. We will first present our methodology and then present our results.

2.1. Methodology

The track wall in three dimensions is represented by a set of points calculated by our program *test* [7–9]. The track wall is computed through several steps. First, the track wall in two dimensions represented by the curve μ as shown in Fig. 2 was calculated. Notations in Fig. 2 are as follows: E is the post-etching surface of the detector and OO' is the particle path, while π, π' and π'' are planes parallel to the detector surface. The three-dimensional track wall is generated by rotating the curve μ around the particle track (OO'axis), a cross-section of which is represented by the circle $AA'$and $B'BB''$.

The 3-D body of the track was first cut by the planes (π, π', π'' and others) which were parallel to the detector surface (horizontal planes in panel (a) of Fig. 2). The intersections between these horizontal planes and the 3-D track are the horizontal semi-elliptical curves η, η', η'', ... (Fig. 2). The number of points that represent the horizontal curves η was kept constant. A mesh of triangles was formed from these points to represent the track wall, which is also schematically shown in Fig. 2. The procedures of forming triangles were applied for the entire track. Some peculiarities arose when triangles were formed between last circle η^n and the tip of the track T. In this case, all triangles have one common point T while the other two points of the triangles are neighbouring points on η^n. To represent the track wall properly, up to 100 horizontal intersections for each track were employed.

The next step is the determination of normal lines for all triangles. For example, a triangle formed by the points $T_1(x_1, y_1, z_1)$, $T_2(x_2, y_2, z_2)$ and $T_3(x_3, y_3, z_3)$ (Fig. 2) is considered. The normal $\vec{n}$ for this triangle is given through the formula

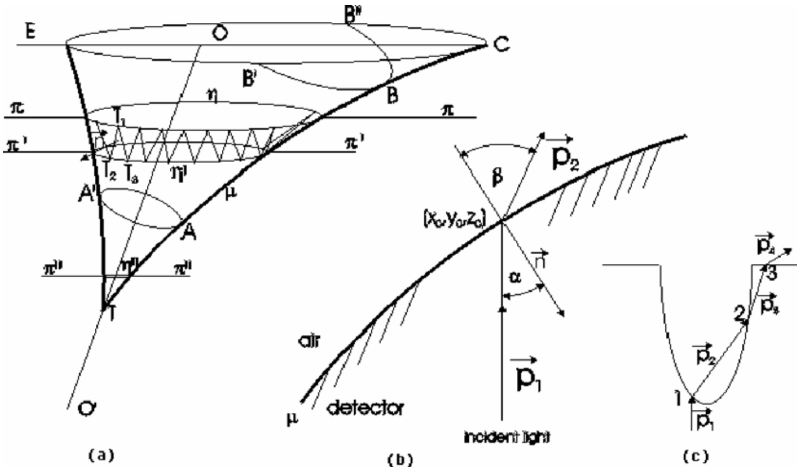

Fig. 2. Panel (a): Construction of the track wall, the horizontal planes π, π' and π'' and the triangular elements on the track wall. Panel (b): Refraction of a light ray at the air-detector interface. Panel (c): A possible path of the light ray in the transmission operation mode of the microscope, i.e. triple refraction. Total reflection is possible at points 1 or 3. The four vectors p_i describe the path of a ray through the track.

$$\vec{n} = \begin{bmatrix} \vec{i} & \vec{j} & \vec{k} \\ x_2 - x_1 & y_2 - y_1 & z_2 - z_1 \\ x_3 - x_1 & y_3 - y_1 & z_3 - z_1 \end{bmatrix}, \tag{1}$$

where $\vec{i}, \vec{j}, \vec{k}$ are unit vectors along the axes of the coordinate system. The vector $\vec{n}$, as defined here, has a direction away from the track core towards the body of the detector and its magnitude should also be normalized to unity.

A ray tracing method based on geometrical optics was used in this work. Here, the transmission operation mode of the microscope is considered. The light comes from the bottom as shown in panel (b) of Fig. 2. The light ray is represented by the vertical line which intersects at the point (x_0, y_0, z_0), which is the *geometrical mean* of a generated triangle, with the track wall (represented by the curve μ). The vector $\vec{p}_1$ represents the direction of incident ray. Here, we assume that all the incident light rays are perpendicular to the general surface of the detector (i.e. regions without tracks). It is not appropriate to assume that the rays come from a cone for such a small object as the track. In addition, the microscope used in our experimental work has a lens between the lamp and the object, which creates a parallel beam of light. The angle between the incident light and the normal line to the surface is α and that between the refracted light and the normal is β. The angle β is determined from the law of refraction as

$$n \sin\alpha = \sin\beta, \tag{2}$$

where n is the refractive index.

The vector $\vec{p}_2$ represents the light ray after refraction, which is determined through the following set of equations:

$$\vec{p}_1 \cdot \vec{p}_2 = \cos(\beta - \alpha), \tag{3}$$

$$\vec{n} \cdot \vec{p}_2 = -\cos\beta, \tag{4}$$

$$(\vec{p}_1 \times \vec{n}) \cdot \vec{p}_2 = 0. \tag{5}$$

The equations for the line describing the new light ray after refraction are

$$\frac{x - x_0}{p_{2x}} = \frac{y - y_0}{p_{2y}} = \frac{z - z_0}{p_{2z}}, \tag{6}$$

where p_{2x}, p_{2y} and p_{2z} are components of the vector $\vec{p}_2$. The reduction of the light intensity due to the refraction on the detector–air surface was calculated by the formula given by Skvarc [5] (as their Eq. (2)).

In some cases, the light ray may return back to the detector. This more complex case is schematically shown in panel (c) of Fig. 2. The new entrance point (denoted by 2) on the track wall has to be determined. Another refraction occurs at that point and a further reduction in the ray intensity has to be determined. A total of three refractions are possible for a light ray (see panel (c) of Fig. 2). In this case, the ray paths through the points 1, 2 and 3 are defined by four vectors, namely, $\vec{p}_1$, $\vec{p}_2$, $\vec{p}_3$ and $\vec{p}_4$, each of them being determined using formulas similar to those given above. At point 3, where the ray comes to the detector–air interface, total internal reflection is also possible.

The brightness of all triangular elements in the track wall were calculated systematically and stored in the computer memory. In contrary to our previous work [6], we do not need the graphical presentation of the track appearance in this work, since we are only using the gray level properties for comparison.

2.2. Statistics on light intensities

For illustration purposes only and for simplicity, we segregated the light intensities (into the "intensity number") by dividing the range from no transmission through the detector (completely dark) to total transmission (completely bright) linearly into 256 intervals, with the intensity number 0 representing completely dark while 255 representing completely bright. The intensity number resembles the gray level obtained from image analysis (see Section 3 below).

As an example, Fig. 3 shows the distribution of intensity numbers obtained by ray tracing for a track from an alpha particle with incident energy of 5 MeV and incident angle of 50°. The distribution is characterized by a large peak for intensity number 0 (completely dark) and a long tail for the larger intensity numbers. The mean and median intensity numbers are 83.075 and zero, respectively. In fact, this distribution is typical for essentially all tracks, except some which have no light transmission at all (see below). Of course, in reality, we expect spreads of light intensities around the peaks and shifts of the gray levels due to noise in the camera or imperfections of the detector, etc. For a comparison, Fig. 3 also shows the distribution of gray levels (obtained by ImageJ analysis, to be described in Section 3 below) of a real track from an alpha particle with incident energy of 5 MeV and incident angle of 50°. Here, a large peak exists with the maximum at gray level of 43. It is likely that this corresponds to a shift from the peak for intensity number 0 obtained from ray tracing.

Table 1 shows some statistics for the light intensity number for tracks from alpha particles with an incident angle of 90° for different incident energies obtained from ray tracing. It is interesting to see that in fact there is no light transmission at all for incident energies at or larger than 4 MeV and light transmission is minimal for most of the other incident energies with the maximum of only about 15% for 1.5 MeV. Therefore, we can see that the light intensity is not useful for distinguishing alpha energies from the tracks for normal incidence. Identification of the alpha energy has to rely on other parameters such as the track opening dimensions.

Table 2 shows some statistics for the light intensity number for tracks from alpha particles with an incident angle of 50° for different incident energies obtained from ray tracing. We can see that the mean intensity numbers are indeed different for different incident alpha energies, so this can be used as a variable for quantitative comparisons. The 80% percentile number has a large spread among different alpha energies so it is also a good variable. Other percentile numbers do not show such a large spread. All median values are zero while all maximum values are 245, so these are not

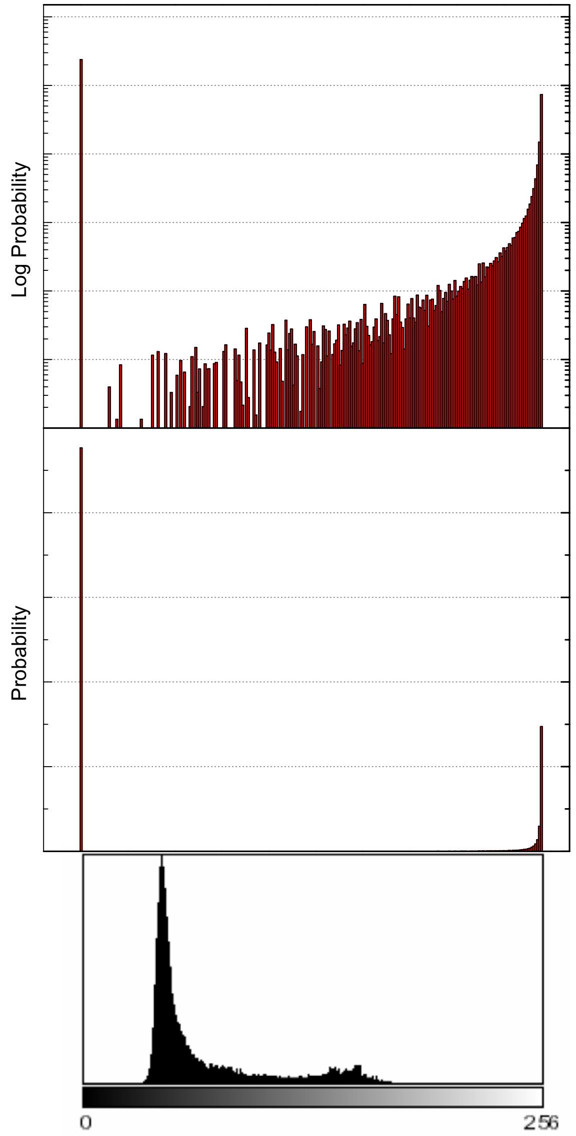

Fig. 3. (Top): Distribution of light intensities obtained by ray tracing for a track from an alpha particle with incident angle of 50° and incident energy of 5 MeV. A log scale has been used for the probability to show more details for lower values of probabilities. (Middle): Same distribution as in the top diagram, but a linear scale has been used for the probability. (Bottom): Distribution of gray levels experimentally obtained by ImageJ analysis for such an alpha particle track.

Table 1
Some statistics for the light intensity number for tracks from alpha particles for different incident energies for incident angle of 90° obtained from ray tracing

Incident alpha energy (MeV)	Expected depth (mm)	Minimum (except 0)	Mean
1.5	3.893	24	39.085
2.0	5.390	66	23.225
2.5	7.012	13	12.262
3.0	8.705	20	4.965
3.5	10.411	149	0.608
4.0	10.027	0	0
4.5	7.195	0	0
5.0	5.137	0	0

Table 2
Some statistics for the light intensity number for tracks from alpha particles for different incident energies for incident angle of 50° obtained from ray tracing

Incident alpha energy (MeV)	Expected depth (μm)	Minimum (except 0)	Mean	80% percentile
1.5	2.463	8	82.589	239
2.0	3.431	6	63.194	232
2.5	4.446	5	51.698	208
3.0	5.458	10	45.544	0
3.5	6.411	21	43.738	0
4.0	6.003	17	52.315	216
4.5	3.833	21	66.901	241
5.0	2.255	15	83.075	245

All median values are zero while all maximum values are 245.

good variables for quantitative comparisons. Moreover, in real experiments, the minimum value (other than zero) is likely obscured by the spread of the peak for no transmission, so this is also not a good variable for quantitative comparisons. Based on these, we thus propose to use the mean and the 80% percentile gray levels from real experiments as quantitative variables to differentiate among tracks.

3. Gray levels of tracks obtained from experiments

3.1. SSNTD Basics

For the present work, we employed CR-39 SSNTDs with a thickness of 1000 μm purchased from Page Mouldings (Pershore) Limited (Worcestershire, England). The CR-39 detectors were cut into pieces with an area of 1 cm × 1 cm.

The cut detectors were irradiated with alpha particles with energies from 1.5 to 5 MeV in steps of 0.5 MeV for the incident angle of 50° (with respect to the detector surface) through a collimator. The alpha source employed in the present study was a planar ^{241}Am source (main alpha energy = 5.49 MeV under vacuum). Normal air was used as the energy absorber to control the final alpha energies incident on the detector. A relationship between the alpha energy and the air distance traveled by an alpha particle was therefore needed. This relationship was obtained by measuring the energies for alpha particles passing different distances through normal air using α spectroscopy systems (ORTEC Model 5030) with passivated implanted planar silicon (PIPS) detectors of areas of 300 mm^2.

After irradiation, the CR-39 detectors were etched in a 6.25 N aqueous solution of NaOH at 70 °C for 6 h. The temperature was kept constant with an accuracy of ±1 °C. The detectors were etched using a magnetic stirrer (Model No. SP72220-26, Barnstead/Thermolyne, Iowa, USA). After chemical etching, the detectors were taken out from the etchant, rinsed with distilled water and dried in air. An optical microscope in the transmission mode was used to view the tracks with the focus on the detector surface. The images were then recorded in the JPEG format by a digital camera (Olympus DP 11) attached to the microscope.

3.2. Gray level determination

In the present studies, two different softwares have been used to determine the gray level properties of the track images. The first one is the free ImageJ (Image Processing and Analysis in Java) software (version 1.29×) (http://rsb.info.nih.gov/ij/). ImageJ is a powerful tool which can perform most image processing or analysis tasks, including measurements of spatial dimensions as well as gray levels. An example of using ImageJ to obtain the gray level properties of tracks from 2 MeV alpha particles with incident angle of 50° is shown in Fig. 4. The captured track image is shown on the left. The track to be analysed has been manually selected (the encircled one). The distribution of gray levels is plotted and the total number of pixels analysed, mean gray level, standard deviation of the gray levels, minimum, maximum and mode of the gray levels are also shown.

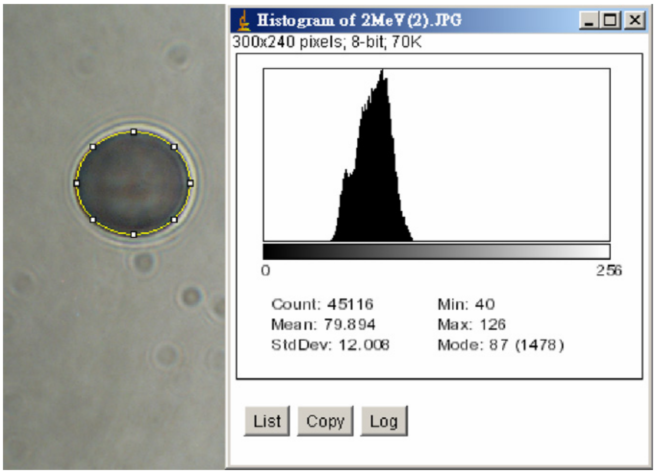

300x240 pixels; 8-bit; 70K

Count: 45116
Mean: 79.894
StdDev: 12.008
Min: 40
Max: 126
Mode: 87 (1478)

Fig. 4. An example of using ImageJ to obtain the gray level properties of tracks from 2 MeV alpha particles with 50° incident angle. Left: A captured track image with the encircled area being analysed. Right: The distribution of gray levels is plotted and the total number of pixels analysed, mean gray level, standard deviation of the gray levels, minimum, maximum and mode of the gray levels are also shown.

The second software used to determine the gray level properties of the track images is the commercially available Adobe® Photoshop® (Adobe® Photoshop® CS and Iamge-Ready CS ver. 8) software. An example of obtaining the gray level properties of tracks from 3 MeV alpha particles with 50° incident angle is shown in Fig. 5. A captured track image is shown on the left. The track to be analysed has been manually selected (the encircled one). The distribution of gray levels is plotted and the total number of pixels analysed, mean gray level, standard deviation of the gray

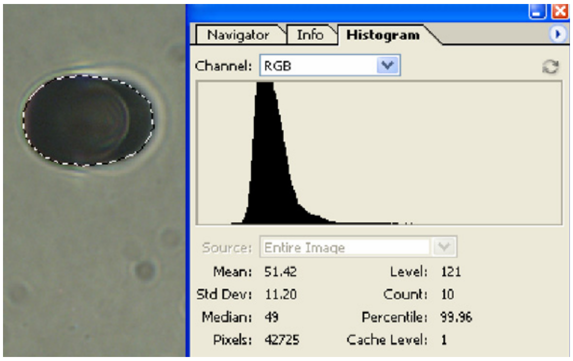

Channel: RGB
Source: Entire Image
Mean: 51.42
Std Dev: 11.20
Median: 49
Pixels: 42725
Level: 121
Count: 10
Percentile: 99.96
Cache Level: 1

Fig. 5. An example of using Adobe® Photoshop® to obtain the gray level properties of tracks from 3 MeV alpha particles with 50° incident angle. Left: A captured track image with the encircled area being analysed. Right: The distribution of gray levels is plotted and the total number of pixels analysed, mean gray level, standard deviation of the gray levels, minimum, maximum and median of the gray levels are also shown.

levels, minimum, maximum and median of the gray levels are also shown.

Table 3
The means, medians, minimum and maximum values and 80% percentile for four measurements of the gray levels of the same alpha track with 2 MeV incident energies and 50° incident angle obtained using Adobe® Photoshop®

Mean	Median	Minimum	Maximum	80% percentile	κ	λ	ε
109.11	110	63	184	124	0.981	0.298	0.304
72.61	73	32	147	83	0.990	0.300	0.300
71.33	71	31	130	83	1.008	0.300	0.298
70.94	71	31	159	79	0.999	0.297	0.293

Also shown are the values of the coefficients κ, λ and ε.

Table 4
The minimum values, means, medians, 80% percentiles, the values of the coefficients κ, λ and ε for alpha tracks with different incident energies and 50° incident angle

Energy (MeV)	Minimum	Mean	Median	80% percentile	κ	λ	ε	Predicted energy (MeV)
1.5	48	97.96	100	113	0.961	0.250	0.289	1.5
	47	107.90	112	125	0.937	0.200	0.263	1.5
	41	94.05	97	112	0.947	0.268	0.321	1.5
2.0	70	109.64	110	124	0.991	0.350	0.359	2.0
	60	107.79	110	123	0.956	0.260	0.304	1.5
	48	86.90	87	100	0.997	0.333	0.336	2.0
	61	102.00	103	116	0.976	0.310	0.333	2.0
2.5	44	88.26	92	102	0.922	0.208	0.286	2.5
	47	91.19	94	105	0.940	0.234	0.294	1.5
	35	69.33	72	80	0.928	0.216	0.288	2.5
3.0	66	97.16	94	106	1.113	0.429	0.316	3.5
	51	81.63	80	91	1.056	0.379	0.323	3.0
	53	83.99	83	94	1.033	0.367	0.334	3.0
3.5	65	89.48	88	97	1.064	0.391	0.327	3.0
	79	98.39	97	103	1.077	0.333	0.256	3.0
	36	61.39	58	70	1.154	0.545	0.391	3.5
	39	61.18	59	60	1.109	0.050	−0.059	4.0
	60	84.05	81	90	1.145	0.429	0.283	3.5
	70	96.61	95	102	1.064	0.280	0.216	3.5
	60	86.03	84	93	1.085	0.375	0.290	3.0
	80	102.30	99	104	1.174	0.263	0.089	4.0
	67	87.09	85	91	1.116	0.333	0.217	3.5
	67	94.44	91	102	1.143	0.458	0.315	3.5
	29	49.55	48	55	1.082	0.368	0.287	3.0
	26	49.47	47	55	1.118	0.381	0.263	3.5
4.0	47	74.02	70	80	1.175	0.435	0.260	4.0
	45	66.76	65	70	1.088	0.250	0.162	3.5
	27	48.23	45	51	1.179	0.333	0.154	4.0
	32	56.90	53	59	1.186	0.286	0.100	4.0
	39	67.98	64	72	1.159	0.320	0.161	4.0
	33	53.88	52	58	1.099	0.316	0.217	3.5
4.5	31	52.88	49	55	1.216	0.333	0.118	4.0
	43	72.45	65	78	1.339	0.591	0.252	4.5
	26	50.07	46	52	1.204	0.300	0.097	4.0
	35	61.36	54	62	1.387	0.421	0.034	4.5
	44	71.87	64	83	1.394	0.950	0.557	5.0
5.0	36	60.88	56	67	1.244	0.550	0.306	5.0
	42	65.98	60	73	1.332	0.722	0.390	5.0
	40	62.31	57	68	1.312	0.647	0.335	5.0

The predicted incident energies by using discriminant analysis with κ, λ and ε as independents are also shown.

The gray level properties given by ImageJ and Adobe® Photoshop® are commensurate with each other. One important difference is that ImageJ gives the mode while Adobe® Photoshop® gives the median. A special feature of Adobe® Photoshop® is that the software can help define and draw the track boundary, so that a smooth outline can be obtained relatively quickly even for non-circular track openings. An example of the outline can also be found on the left panel of Fig. 5. The gray level corresponding to a particular percentile can also be determined using Adobe® Photoshop®.

3.3. Consistency of gray level measurements

As described in Section 2.2, we propose to use the mean and the 80% percentile gray levels as variables to differentiate among tracks. However, before quantitative comparisons can be made for the gray level properties of the tracks, it is important to check and ensure that the properties being used for comparison should be self-consistent, i.e. the properties for the same tracks (same incident energy and angle) should be invariant among different exposures and image analyses.

Table 3 shows the gray level properties for four measurements of the gray levels of the same track from an alpha particle with 2 MeV incident energy and 50° incident angle obtained using Adobe® Photoshop®. The gray level properties vary greatly among the four measurements. This can be due to different illumination of the microscope or exposure of the digital camera, etc. With such inconsistencies, it is impossible to make meaningful quantitative comparisons of the gray level properties for alpha tracks with different energies or angles.

We try to propose some variables, which are invariant among different exposures, through normalization with the spread in gray levels, i.e. Median gray level – Minimum gray level, or in short (Median – Min). Regarding the quantitative variable involving the mean gray level, we propose to use the coefficient κ [= (Mean – Min)/(Median – Min)]; and regarding the quantitative variable involving the 80% percentile gray level, we propose to use the coefficient λ [= (80% percentile – Median)/(Median – Min)]. We also introduce a third coefficient ε [= (80% percentile – Mean)/(Median – Min)] to study the difference between the mean and the 80% percentile gray levels. The coefficients κ, λ and ε values have been calculated and shown in Table 3. It is interesting to see that these coefficients are very consistent for the same alpha particle track despite that the gray level properties are very different.

3.4. Results for tracks from alpha particles with 50° incident angle and different incident energies

Table 4 shows the minimum values, means, medians, 80% percentiles, the values of the coefficients κ, λ and ε for alpha tracks with different incident energies and 50° incident angle. From these data, the variations between the coefficients κ, λ and ε with the track depth (μm) are shown in Fig. 6. It can be seen that the track depths cannot be predicted by any one of these coefficients. However, a three-dimensional scatter plot of the coefficients κ, λ and ε for, as shown in Fig. 7, show that the alpha tracks with different incident energies are separated relatively clearly. This hints that the use of multivariate analyses might help separate the alpha tracks with different energies. As an example, the scatter plot of factor scores (from factor analysis using κ, λ and ε as the variables) is shown in Fig. 8. Again, the alpha tracks with different incident energies are separated relatively clearly. The predicted incident energies by using discriminant analysis with κ, λ and ε as independents are also shown in Table 4. It can be seen that effectively all alpha energies can be determined with an accuracy of ±0.5 MeV. This is a very good result considering the relatively small sample size.

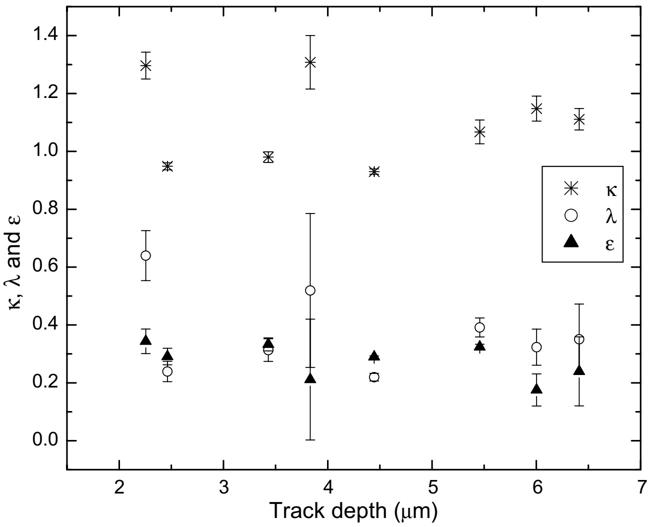

Fig. 6. The variation between the coefficients κ, λ and ε with the track depth (μm) for alpha tracks with different incident energies and 50° incident angle.

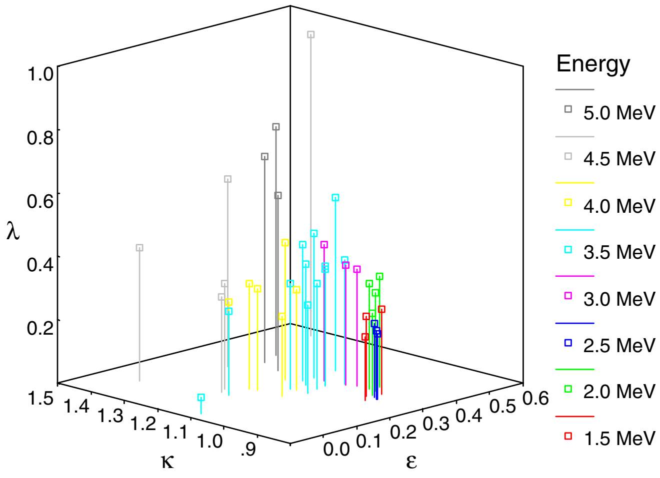

Fig. 7. The three-dimensional scatter plot of the coefficients κ, λ and ε for alpha tracks with 50° incident angle and different incident energies.

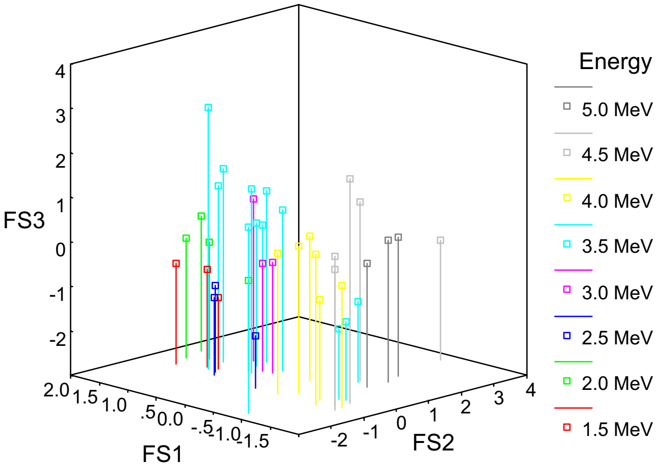

Fig. 8. The three-dimensional scatter plot of the factor scores for alpha tracks with 50° incident angle and different incident energies.

4. Conclusions

(1) A ray tracing method based on geometrical optics was used to study the tracks from alpha particles with energies from 1.5 to 5 MeV (with steps of 0.5 MeV) and with incident angles of 90° and 50°. The transmission operation mode of the microscope is considered. We have found that light intensity is not useful for distinguishing alpha energies from the tracks for 90° incidence because of no or weak light transmission through the tracks. From the results for 50° incidence and considering the distribution of light intensities from the tracks, the mean and the 80% percentile gray levels from real experiments are proposed as quantitative variables to differentiate among tracks.

(2) The gray level properties for the same track for different exposures vary to large extents. We introduce three variables to make empirical corrections, viz., κ [= (Mean − Min)/(Median − Min)], λ [= (80% percentile − Median)/(Median − Min)] and ε [= (80% percentile − Mean)/(Median − Min)]. It is interesting to see that these coefficients are very consistent for the same alpha particle track despite that the gray level properties are very different.

(3) Gray level results have been obtained for tracks from alpha particles with 50° incident angle and different incident energies. The track depths cannot be predicted by any one of the coefficients κ, λ and ε. Multivariate analyses can help separate the alpha tracks with different energies. By using discriminant analysis with κ, λ and ε as independents, effectively all alpha energies can be determined with an accuracy of ±0.5 MeV.

Acknowledgement

The present research is supported by the CERG grant CityU 102803 from the Research Grant Council of Hong Kong.

References

[1] D. Nikezic, K.N. Yu, Mater. Sci. Eng. R 46 (2004) 51.
[2] A.P. Fews, Nucl. Instr. and Meth. B 72 (1992) 91.
[3] J. Skvarc, R. Ilic, A. Kodre, Nucl. Instr. and Meth. B 71 (1992) 60.
[4] M.P.M. Assunção, R. Pugliesi, M. De Menezes, Appl. Radiat. Isot. 45 (1994) 851.
[5] J. Skvarc, Radiat. Meas. 31 (1999) 217.
[6] D. Nikezic, F.M.F. Ng, C.W.Y. Yip, K.N. Yu, Radiat. Meas. 40 (2005) 375.
[7] D. Nikezic, K.N. Yu, Radiat. Meas. 37 (2003) 39.
[8] D. Nikezic, K.N. Yu, Radiat. Meas. 37 (2003) 595.
[9] D. Nikezic, K.N. Yu, Comput. Phys. Commun. 174 (2006) 160.